

# Proportional-integral-derivative-acceleration robust controllers for vibrating systems

Journal of Vibration and Control  
2022, Vol. 0(0) 1–11  
© The Author(s) 2022  
Article reuse guidelines:  
[sagepub.com/journals-permissions](https://sagepub.com/journals-permissions)  
DOI: 10.1177/10775463211060898  
[journals.sagepub.com/home/jvc](https://journals.sagepub.com/home/jvc)  
SAGE

Danielle S Gontijo<sup>1</sup> , José M Araújo<sup>2</sup> , Tito LM Santos<sup>3</sup>, and Fernando O Souza<sup>4</sup> 

## Abstract

This paper presents a design framework to obtain a robust multivariable Proportional-Integral-Derivative (PID) controller for second-order linear vibrating systems. A Proportional-Integral-Derivative plus acceleration (PIDA) controller is also proposed to deal with the regularization problem. Relevant control challenges, such as modeling error, regulatory performance optimization, regional pole placement, saturation avoidance, and constant reference tracking are handled within the proposed Linear Matrix Inequality (LMI) design approach. The design strategy is obtained from a linear transformation that can be applied to achieve constant reference tracking for an actuated subspace of underactuated systems. Moreover, the integral action has two additional objectives: (1) to improve regulatory performance in the presence of constant disturbance and (2) to increase the design degree of freedom in order to robustly achieve closed-loop specifications. Three simulation case studies are used to highlight the benefits of the PID and PIDA controllers.

## Keywords

proportional-integral-derivative controller; acceleration feedback; robust control; linear matrix inequalities

## 1. Introduction

The control of systems that exhibit vibratory behavior has received increased attention in the last decades. Nowadays, the active or semi-active control of such systems is widely applied from skyscraper stabilization under wind gusts to small applications such as microelectromechanical accelerometers, jerk control, flexible structures of aircraft, and the active suspension of vehicles or seats (Alfadhli et al., 2018; Hayati et al., 2020; Singh et al., 2019). In these problems, the success of the designed system depends upon a series of requirements, for instance, the robustness of the controlled system against a model mismatch, disturbance rejection in track control problems, and saturation avoidance of the control effort. For both of the more used modeling approaches, namely, finite-element models (FEM) (Zhang and Li 2013) and the receptance approach (Mottershead et al., 2008; Ram and Mottershead, 2013; Zhu et al., 2009), the modeling errors are unavoidable, given the approximate nature of the former and the experimental appeal on the latter. Nonlinear behavior is also an important source of uncertainty. Motivated by the relevance of modeling error, some studies on the robustness analysis and design of the controlled system have been delivered in recent times. The robust control of vibrating systems using

FEM or receptance models can be addressed by different approaches (Abdelaziz, 2013; Adamson et al., 2020; Franklin et al., 2021). The partial eigenstructure assignment with guaranteed robustness is described in early and more recent works as Cai et al. (2010); Araújo et al. (2018); Xie (2021). Since uncertainties must be taken into account in some step of the design to avoid unexpected system instability in closed-loop, they are a prominent issue for the design of vibration control systems.

The disturbance rejection problem in the context of vibration control is another relevant issue in applications as

<sup>1</sup>Programa de Pós-graduação em Engenharia Elétrica, Universidade Federal de Minas Gerais, Brazil

<sup>2</sup>Grupo de Pesquisa em Sinais e Sistemas, Instituto Federal da Bahia, Brazil

<sup>3</sup>Departamento de Engenharia Elétrica, Universidade Federal da Bahia, Brazil

<sup>4</sup>Departamento de Engenharia Eletrônica, Universidade Federal de Minas Gerais, Brazil

Received: 1 June 2021; revised: 27 September 2021; accepted: 30 October 2021

### Corresponding author:

Fernando O. Souza, Departamento de Engenharia Eletrônica, Universidade Federal de Minas Gerais, Belo Horizonte-MG, 31.270-901, Brazil. Email: [fosouza@ufmg.br](mailto:fosouza@ufmg.br)

structural control. In Gudarzi (2015) the aforesaid problem is dealt by estimating unknown disturbances in the context of seismic alleviation in buildings. Applications of piezoelectric actuators for disturbance rejection in the control of thin-walled and other smart structures are addressed in Zhang et al. (2014, 2019, 2021).

Besides that, acceleration feedback can be a requirement for systems with considerable mass imbalance (Acevedo et al., 2020) or even in the case of a singular mass matrix (Abdelaziz, 2015). Infinite eigenstructures imply very high acceleration or jerk impulses that can cause injuries in humans or animals, see for instance Hayati et al. (2020). Then, regularizing the mass matrix via acceleration feedback is often a need.

Linear matrix inequalities (Boyd et al., 1994; Chilali and Gahinet, 1996) can be successfully applied in control problems that involve multiple requirements, as robustness, guaranteed cost disturbance attenuation, and regional pole placement, among others (de Almeida and Araújo, 2019; Li et al., 2013; Richiedei and Tamellini, 2021).

This type of design and analysis formulations has also received increasing attention in mechanical systems applications (Hiramoto and Grigoriadis, 2016; Guo et al., 2020).

Due to the convexity nature of the formulation, several control challenges can be combined such as regional pole placement, robust stability, and guaranteed robust performance for uncertain or time-varying systems, null tracking error in the presence of constant disturbance, saturation avoidance, among others relevant issues.

This paper presents a robust framework to design multi-variable Proportional-Integral-Derivative (PID) or, when necessary, Proportional-Integral-Derivative-Acceleration (PIDA) controllers for parametric uncertain second-order vibrating systems. In contrast to related works based only on proportional and derivative feedback, the integral action is used to achieve null set-point tracking error in the presence of constant disturbance with respect to the actuated degrees-of-freedom and to increase the design flexibility. The acceleration action may be used to deal with the regularization problem, which is one of the contributions of this paper. The design methodology is based on regional pole placement also known as  $D$ -stability,  $H_\infty$  performance, stabilization of asymmetric systems, regularization problem, actuator saturation avoidance, and set-point tracking, which are jointly handled within the linear matrix inequality (LMI) framework.

## 2. Notation

Let the scalar  $j = \sqrt{-1}$  and  $\mathbb{R}^{m \times n}$  be the set of  $m \times n$  real matrices. If  $s$  is a complex number,  $\text{Re}(s)$  denotes its real part and  $\text{Im}(s)$  its imaginary part. For a matrix,  $X$  denotes its transpose by  $X^T$  and its inverse by  $X^{-1}$ . If  $X$  is square and symmetric then  $X > 0$ , ( $X \geq 0$ ) indicates that  $X$  is positive

(semi) definite; similarly,  $X < 0$  ( $X \leq 0$ ) indicates that  $X$  is negative (semi) definite. The notation  $\text{cov}$  denotes convex hull and  $\text{diag}\{x_1, \dots, x_n\}$  is used for a diagonal matrix whose diagonal entries, starting in the upper left corner, are  $x_1, \dots, x_n$ . Moreover, for any square matrix  $X$ , we define the operator  $\text{sm}\{X\} = X + X^T$ . Let  $I_n$  ( $0_n$ ) be the identity (zero) matrix with dimension  $n \times n$  and  $0_{n \times m}$  the zero matrix with dimension  $n \times m$ ; throughout the paper such subscripts will be suppressed, whenever the dimension is clear from the context.

### 2.1. Problem formulation

Consider the class of vibrating systems described by the second-order linear model

$$M(t)\ddot{z}(t) + D(t)\dot{z}(t) + S(t)z(t) = B(t)u(t) + F(t)w(t) \quad (1)$$

where  $z(t) \in \mathbb{R}^n$  is the state vector,  $u(t) \in \mathbb{R}^m$  is the control input, and  $w(t) \in \mathbb{R}^p$  is the exogenous disturbance vector.  $M(t)$ ,  $D(t)$ ,  $S(t) \in \mathbb{R}^{n \times n}$  are, respectively, the mass, damping and stiffness matrices, and  $B(t) \in \mathbb{R}^{n \times m}$ ,  $F(t) \in \mathbb{R}^{n \times p}$  are, respectively, the control and disturbance matrices. Since in engineering applications, it is now very common that the system under investigation is not known exactly, that is, the system contains some elements which are uncertain, in (1) the system matrices are given by the values of parameter uncertainties at time  $t$  and it is assumed that they belong to the polytopic set

$$\Omega := \text{cov} \left\{ \begin{bmatrix} M_1 & D_1 & S_1 \\ B_1 & F_1 & 0 \end{bmatrix}, \begin{bmatrix} M_2 & D_2 & S_2 \\ B_2 & F_2 & 0 \end{bmatrix}, \dots, \begin{bmatrix} M_N & D_N & S_N \\ B_N & F_N & 0 \end{bmatrix} \right\} \quad (2)$$

with vertices defined by the extreme values of the parameters uncertainties.

The control signal  $u(t)$  is an extension of the single-variable PIDA controller to the multivariable case, as so the proportional control action (P) is proportional to the current error. The integral action (I) can eliminate the steady-state offset and the derivative action (D) is specially related with shaping the damping behavior of the closed-loop system. Finally, we use the acceleration action (A) to avoid impulsive behavior in the closed-loop system, see Example 2 for illustration of this point. Thus, the multivariable PIDA controller is defined by

$$u(t) = K_P e(t) + K_I \int_0^t e_a(\tau) d\tau + K_D \dot{e}(t) + K_A \ddot{e}(t), \quad (3)$$

with  $e(t) = z(t) - r(t)$  where  $r(t) \in \mathbb{R}^n$  is the desired set-point vector, and  $e_a(t)$  denotes the error signal on the actuated states; in the case of full actuated systems  $e_a(t) = e(t)$ , otherwise,  $e_a(t) = Ue(t) \in \mathbb{R}^a$ , for an appropriated binary

matrix  $U \in \mathbb{R}^{a \times n}$ , such that  $e_a(t)$  is composed only by the entries of  $e(t)$  resulting from the actuated states. In addition,  $K_P, K_D, K_A \in \mathbb{R}^{m \times n}$  and  $K_I \in \mathbb{R}^{m \times a}$ . Notice that we cannot have perfect tracking of arbitrary constant reference in the underactuated case, even in the absence of disturbance, due to the control action limitation. Thus, the actuated error, namely  $e_a(t)$ , is defined in order to ensure trajectory tracking on the actuated degrees-of-freedom.

In order to enjoy from the LMI framework to design the robust controller we rewrite the system (1) such that the PID part of the controller (3) becomes a static state feedback controller. In view of that we define the following state variables

$$x_1(t) = z(t), \quad x_2(t) = \dot{z}(t), \quad x_3(t) = -\int_0^t e_a(\tau) d\tau \quad (4)$$

that yield the following feedback augmented descriptor model

$$E(t)\dot{x}(t) = A(t)x(t) + B_u u(t) + B_w(t)w(t) + ([0_n \quad 0_n \quad -U]^T r(t) + (B(t)K_A)\ddot{r}(t)) \quad (5.1)$$

$$u(t) = Kx(t) - K \begin{bmatrix} r^T(t) & \dot{r}^T(t) & 0_{1 \times a} \end{bmatrix}^T \quad (5.2)$$

$$y(t) = Cx(t) \quad (5.3)$$

with  $x^T(t) = [x_1^T(t) \quad x_2^T(t) \quad x_3^T(t)]$ ,

$$A(t) = \begin{bmatrix} 0_n & I_n & 0_{n \times a} \\ -S(t) & -D(t) & 0_{n \times a} \\ U & 0_{a \times n} & 0_a \end{bmatrix}, \quad (6)$$

$$B_u(t) = \begin{bmatrix} 0_{n \times m} \\ B(t) \\ 0_{a \times m} \end{bmatrix}, \quad B_w(t) = \begin{bmatrix} 0_{n \times p} \\ F(t) \\ 0_{a \times p} \end{bmatrix},$$

$$E(t) = \text{diag}\{I_n, (M(t) - B(t)K_A), I_a\},$$

$$K = [K_{Pm \times n} \quad K_{Dm \times n} \quad K_{Im \times a}],$$

$$C = [I_n \quad 0_n \quad 0_{n \times a}].$$

Accordingly, with respect to Equation (2), in the case of uncertainties, the uncertain descriptor model matrices belong to the polytopic set

$$\Omega_D := \text{cov} \left\{ \begin{bmatrix} E_1 & A_1 \\ B_{u,1} & B_{w,1} \end{bmatrix}, \begin{bmatrix} E_2 & A_2 \\ B_{u,2} & B_{w,2} \end{bmatrix}, \dots, \begin{bmatrix} E_N & A_N \\ B_{u,N} & B_{w,N} \end{bmatrix} \right\}, \quad (7)$$

The proposed PIDA controller is defined by a linear time-invariant control law. Hence, standard tools for

robustness analysis with respect to unstructured uncertainties and delays can be applied *a posteriori* (Franklin et al., 2021). Moreover, due to the generality of the polytopic description, polytopic difference inclusions can be used to formally represent time-varying delay effect (Gielen et al., 2010) and some types of nonlinearities (Boyd et al., 1994; Hu et al., 2006) *a priori*. In this last case, the robustness against the polytopic uncertainty is handled directly during design stage.

In this paper we will consider two cases accordingly with the mass matrix  $M(t)$  singularity:

Case i)  $M(t)$  is non-singular: we tune a standard PID controller setting  $K_A = 0$  in (3);

Case ii)  $M(t)$  is singular: we design  $K_A$  such that  $(M(t) - B(t)K_A)$  is non-singular, which is possible whenever  $(M(t), B(t))$  has full row rank (Bender and Laub, 1987).

Therefore, in both cases we have that  $(M(t) - B(t)K_A)$  is non-singular and the descriptor model above reduces to a standard state-space description left multiplying (5.1) by  $E(t)^{-1}$ . This explain the reason why the proposed controller (3) has term  $K_A \ddot{r}(t)$ , which can be removed from the control law when the system mass matrix  $M(t)$  is non-singular.

Thus, the control problem under consideration can be stated as follows.

**Problem 1.** Design a PID or PIDA controller for the second-order vibrating linear system in (1) such that the closed-loop system model can be written as a standard state-space description, guaranteeing the existence and uniqueness of state responses and avoiding impulsive behavior that may cause degradation in performance; and for any combination of the following requirements:

- i) The closed-loop poles belong to a prescribed stable region ( $D$ -region) on the complex plane as depicted in Figure 1;
- ii) The  $H_\infty$  performance condition is satisfied for a given disturbance attenuation level  $\gamma > 0$

$$\sup_{\|w(t)\|_2 \neq 0} \frac{\|y(t)\|_2}{\|w(t)\|_2} < \gamma; \quad (8)$$

- iii) The control signal is bounded in amplitude by a given scalar  $u_{\max} > 0$  and a set of initial conditions

$$\max_{t \geq 0} \|u(t)\| \leq u_{\max}. \quad (9)$$

The design requirements listed in the above problem are linked to the system closed-loop behavior and performance. The item i) is related to the desired closed-loop time response that often can be achieved by assigning the

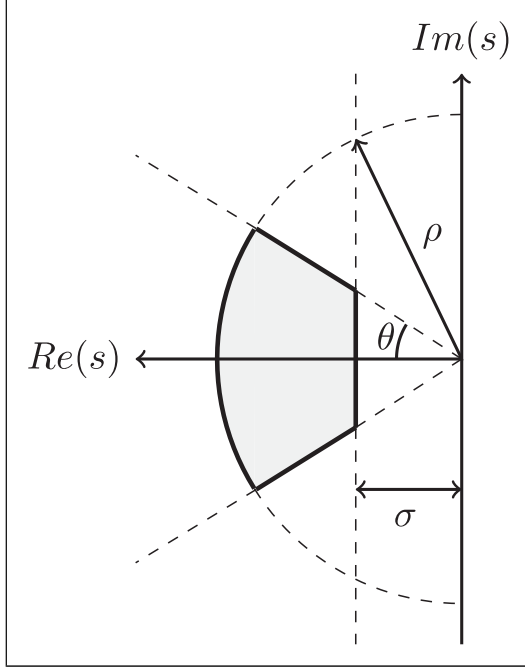


**Figure 1.** D-region for pole placement where is a complex number.

closed-loop poles into a suitable subregion of the complex left-half plane. The  $H_\infty$  performance in item ii) characterizes the worst-case ratio,  $\gamma$ , of the energies contained in the output and the exogenous disturbance input of the system. In contrast, item iii) is concerned in maintaining the linear behavior of the closed-loop system avoiding control-signal saturation and eventual loss of stability by guaranteeing an upper bound on the norm of the control input  $u_{\max}$ .

It is important to close this section by mentioning that the main shortcoming of the proposed strategy is the full-state knowledge assumption. This requirement can be relaxed by using state observers. Also notice that displacement derivative may be directly measured or estimated from the direct displacement information. In the case when  $M$  is non-singular, *Case i*), acceleration feedback is not used, but otherwise the acceleration state may be estimated or entirely measured due to the interesting properties of accelerometers (Abdelaziz, 2015).

## 2.2. Main results

In order to guarantee that  $E(t)$  in (5) is non-singular, in the case when the mass matrix  $M(t)$  is singular, we present the next lemma.

**Lemma 1.** The matrix  $(M(t) - B(t)K_A)$  is non-singular if there exist a nonzero scalar  $\beta$  and a matrix  $K_A \in \mathbb{R}^{m \times n}$  such that

$$\begin{bmatrix} \frac{1}{2}(M_i + M_i^T - B_i K_A - K_A^T B_i^T) & \beta I \\ \beta I & I \end{bmatrix} > 0, \quad (10)$$

for  $i = 1, 2, \dots, L$ , where  $L$  is the number of vertices of the polytopic set  $\Omega$  in (2) keeping the matrices  $M_i$  and  $B_i$  and removing the others. Furthermore if (10) holds then the minimum eigenvalue of  $\text{sm}\{\frac{1}{2}(M(t) - B(t)K_A)\}$  is greater than  $\beta^2$ .

**Proof.** The lemma follows by an application of Theorem 1 in Datta (2017) that yields

$$\begin{bmatrix} \frac{1}{2}(M(t) + M(t)^T - B(t)K_A - K_A^T B(t)^T) & \beta I \\ \beta I & I \end{bmatrix} > 0.$$

Therefore, the conditions in the Lemma are obtained by recalling that to ensure an LMI condition over an entire polytopic uncertain domain, it suffices to check the LMI at the vertices of the convex polytope.

In the case system (1) is free of parametric uncertainties and  $E(t)$  in (5) is non-singular; a myriad of LMI conditions from the literature can be applied directly in the system (5). However, in the presence of uncertainties the space-state description of the model (5) may require inversion of uncertain matrices which is a hard problem in general. Therefore, in the following we present tractable LMI conditions, which do not require inverses of uncertain matrices. The next theorem presents LMI conditions to design a controller PID/PIDA with prescribed closed-loop  $H_\infty$  performance.

**Theorem 1.** Let  $\gamma > 0$  be a prescribed closed-loop  $H_\infty$  performance and  $K_A$  be a given matrix such that  $E(t) = (M(t) - B(t)K_A)$  is non-singular, see Lemma 1. The system (1) in closed-loop with the controller (3) is robustly stable with disturbance attenuation  $\gamma$  if there exist a symmetric matrix  $P \in \mathbb{R}^{2n+a \times 2n+a}$  and a matrix  $Y \in \mathbb{R}^{m \times 2n+a}$  such that  $P > 0$  and

$$\begin{bmatrix} \text{sm}\{A_i P E_i^T + B_{u,i} Y E_i^T\} & E_i P C^T & B_{w,i} \\ C P E_i^T & -\gamma^2 I & 0 \\ B_{w,i}^T & 0 & -I \end{bmatrix} < 0, \quad (11)$$

for  $i = 1, \dots, N$  where  $N$  is the number of vertices of the polytopic set  $\Omega$  in (7). In affirmative case, the controller gains are given in  $K = YP^{-1}$ .

**Proof.** As established in the previous section, the theorem statement is equivalent to design a controller of the form  $u(t) = Kx(t)$  such that the descriptor model (5) in closed-loop is robustly stable with  $H_\infty$  disturbance attenuation level  $\gamma$ . Moreover, assuming that  $E(t)$  is non-singular, consider the

state-space description obtained from system (5) left-multiplying the first equation in (5) by  $E(t)^{-1}$ . Then such design problem can be formulated as the following matrix inequalities (Boyd et al., 1994, Section 6.3.2)

$$\begin{aligned} P > 0, \\ \begin{bmatrix} \text{sm}\{P(E_i^{-1}(A_i + B_{u,i}K))^T\} + E_i^{-1}B_{w,i}(E_i^{-1}B_{w,i})^T & PC^T \\ CP & -\gamma^2 I \end{bmatrix} < 0, \end{aligned} \quad (12)$$

for  $i = 1, \dots, N$ , vertices of the polytopic uncertain domain. Now defining the linearizing variable  $Y = KP$  and applying Schur complement the last inequality is equivalent to

$$\begin{bmatrix} \text{sm}\{E_i^{-1}(A_iP + B_{u,i}Y)\} & PC^T & E_i^{-1}B_{w,i} \\ CP & -\gamma^2 I & 0 \\ B_{w,i}^T(E_i^{-1})^T & 0 & -I \end{bmatrix} < 0, \quad (13)$$

then pre- and post-multiplying it by  $\text{diag}\{E_i, I, I\}$  and its transpose, respectively, the conditions in the theorem are obtained.

The next theorem considers the standard D-region given by the intersection of regions: (i) half-plane  $\text{Re}(s) < -\sigma$ , (ii) conic sector with apex at the origin and inner angle  $2\theta$ , and (iii) disk with radius  $\rho$  and center at the origin, as depicted in Figure 1. The following theorem details how the pole placement in a given D-region can be done via PID/PIDA design.

**Theorem 2.** Let be given a D-region specified by the positive scalars  $\sigma, \rho, \theta$  and a matrix  $K_A$  such that  $E(t) = M(t) - B(t)K_A$  is non-singular, see Lemma 1. The system (1) is D-stable in closed-loop with the controller in (3), that is, the poles of the closed-loop system belong to the D-region depicted in Figure 1, if and only if there exist a symmetric positive matrix  $P \in \mathbb{R}^{2n+a \times 2n+a}$  and a matrix  $Y \in \mathbb{R}^{m \times 2n+a}$  such that

$$\begin{aligned} 2\sigma E_i P E_i^T + A_i P E_i^T + E_i P A_i^T \\ + B_{u,i} Y E_i^T + E_i Y^T B_{u,i}^T < 0, \end{aligned} \quad (14)$$

$$\begin{bmatrix} -\rho E_i P E_i^T & A_i P E_i^T + B_{u,i} Y E_i^T \\ E_i P A_i^T + E_i Y^T B_{u,i}^T & -\rho E_i P E_i^T \end{bmatrix} < 0, \quad (15)$$

$$\begin{bmatrix} \sin \theta (\Theta_i + \Theta_i^T) & \cos \theta (\Theta_i - \Theta_i^T) \\ \cos \theta (\Theta_i^T - \Theta_i) & \sin \theta (\Theta_i + \Theta_i^T) \end{bmatrix} < 0, \quad (16)$$

with  $\Theta_i = A_i P E_i^T + B_{u,i} Y E_i^T$ , for  $i = 1, 2, \dots, V$ , where  $V$  is the number of vertices of the polytopic set  $\Omega$  in (7)

removing  $B_{w,i}$ . In affirmative case, the controller gains are given in  $K = YP^{-1}$ .

**Proof.** Based on the problem formulation in previous section, and assuming that  $E(t)$  is non-singular, consider the state-space description obtained from system (5) left-multiplying the equation (5.1) by  $E(t)^{-1}$ . Then, by an application of Theorem 2.2 from Chilali and Gahinet (1996) in the closed-loop matrix  $E(t)^{-1}(A(t) + B_u(t)K)$ , we have that

$$2\sigma P + Y(t) + Y(t)^T < 0, \quad \begin{bmatrix} -\rho P & Y(t) \\ Y(t)^T & -\rho P \end{bmatrix} < 0,$$

$$\begin{bmatrix} \sin \theta (Y(t) + Y(t)^T) & \cos \theta (Y(t) - Y(t)^T) \\ \cos \theta (Y(t)^T - Y(t)) & \sin \theta (Y(t) + Y(t)^T) \end{bmatrix} < 0,$$

with  $Y(t) = E(t)^{-1}(A(t) + B_u(t)K)P$ . Therefore, the conditions in the theorem are obtained defining the linearizing variable  $Y = KP$ , pre- and post-multiplying the first LMI by  $E(t)$  and  $E(t)^T$ , respectively, and the other ones by  $\text{diag}\{E(t), E(t)\}$  and its transpose, and recalling that to ensure the resulting LMI conditions over the entire polytopic uncertain domain, it suffices to check the LMIs at the vertices of the convex polytope.

Finally, the last LMI condition considers the physical limitation on the maximum control signal amplitude.

**Lemma 2.** (Boyd et al., 1994, Section 7.2.3) Assume the control signal  $u(t) = Kx(t) = YP^{-1}x(t)$  and the initial condition  $x(0)$ . Then  $\max_{t \geq 0} \|u(t)\| \leq u_{\max}$ , if

$$\begin{bmatrix} 1 & x(0)^T \\ x(0) & P \end{bmatrix} \geq 0 \quad \text{and} \quad \begin{bmatrix} P & Y^T \\ Y & u_{\max}^2 I_m \end{bmatrix} \geq 0. \quad (17)$$

Finally, taking into account the above development, the robust PID/PIDA controller design procedure is summarized next.

**Procedure 1.** PID/PIDA controller design for solving Problem 1:

- Step 1: Rewrite the second-order linear vibrating system (1) as the augmented descriptor model (5.1);
- Step 2: Set the  $H_\infty$  performance  $\gamma$ , the control input constraint  $u_{\max}$  (if any), and the desired D-region for the closed-loop pole placement defined by the triplet  $(\sigma, \theta, \rho)$  accordingly with Figure 1;
- Step 3: If the matrix  $M(t)$  is singular find the gain  $K_A$  by solving the LMIs presented in Lemma 1, otherwise set  $K_A = 0$  and go to the next step;
- Step 4: Find the solution  $(P, Y)$  that solves simultaneously the LMI conditions presented in Theorems 1, 2, and Lemma 2;
- Step 5: The PID controller parameters are given in  $K = [K_P \ K_D \ K_I]$  where  $K = YP^{-1}$ .



### 2.3. Numerical examples

In this section are presented two numerical examples drawn from the literature to illustrate and validate the proposed robust PID/PIDA controller design method.

**Example 1.** Consider the active suspension of a car seat sketched in Figure 2 drawn from Reithmeier and Leitmann (2003). This model has been successfully used to design controllers for vehicle active suspension (Pan and Sun, 2019; Sun et al., 2015), vehicle driver seat (Alfadhli et al., 2018; Tu et al., 2021), or for a combination of them as in Reithmeier and Leitmann (2003). The model consists of the car mass ( $m_c$ ) and driver-plus-seat mass ( $m_s$ ). The vibrations are partially mitigated by the shock absorbers at the car and at the seat whose stiffness ( $k_1$  and  $k_2$ ) and damping ( $b_1$  and  $b_2$ ) that can be adjusted by  $u_1(t)$  and  $u_2(t)$ , respectively. The system model is given by (1) with data

$$M = \text{diag}\{m_s, m_c\}, \quad B = I_{2 \times 2}, \quad \text{and} \quad F = \text{diag}\{0, 1\},$$

$$D = \begin{bmatrix} b_2 & -b_2 \\ -b_2 & b_1 + b_2 \end{bmatrix}, \quad S = \begin{bmatrix} k_2 & -k_2 \\ -k_2 & k_1 + k_2 \end{bmatrix}$$

where  $m_c = 1500$  kg and  $m_s \in [70, 120]$  kg (according to the driver's weight),  $k_1 = 4 \times 10^4$  N/m,  $k_2 = 5000$  N/m,  $b_1 = 4000$  N-sec/m and  $b_2 = 500$  N-sec/m. Further, this system can be modeled as (5) by setting  $U = B_T$ .

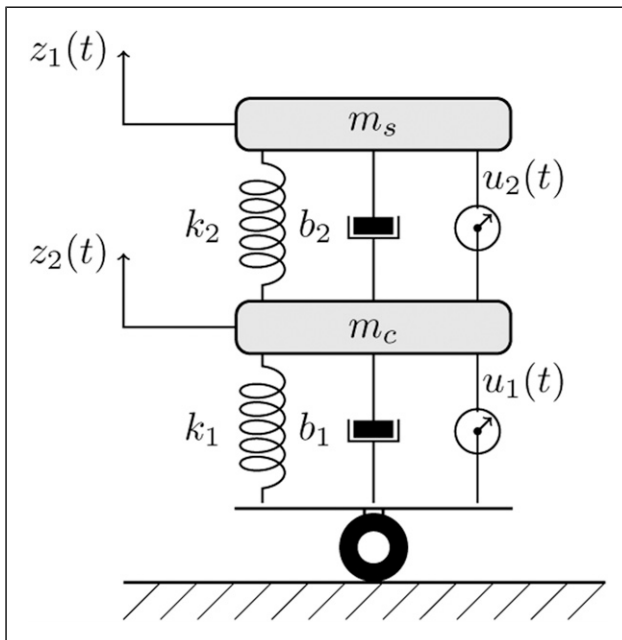


**Figure 2.** The quarter-vehicle model of active suspension system. Example 1.

In this example, the control specifications are: (i) limitation on the control signal amplitude as in (9) with  $u_{\max} = 40000$  for initial condition  $x(0) = [-0.1 \ -0.1 \ 0.09 \ 0.09 \ 0.05 \ 0.05]^T$ , (ii)  $H_\infty$  disturbance attenuation level  $\gamma = 0.1732$  and (iii) the system closed-loop pole placement in the D-region defined as the intersection of the half-plane  $\text{Re}(s) < -0.9$ , a conic sector centered at the origin and with inner angle given by  $\theta = \pi/3$ , and a disk with radius  $\rho = 15$  as shown in Figure 1. Then, following Procedure 1 yields the PID controller gains

$$K_P = \begin{bmatrix} -5748 & -3723 \\ -4844 & -7029 \end{bmatrix}, \quad K_D = \begin{bmatrix} -1090 & -567 \\ -485 & -9837 \end{bmatrix},$$

$$K_I = \begin{bmatrix} -11803 & 1676 \\ -4838 & -46515 \end{bmatrix}.$$

For the results analysis, Figure 3 shows the open- and closed-loop system poles for all integer admissible values of  $m_s$  where the shaded area indicates the desired D-region for the system closed-loop pole placement. Moreover, for  $m_s = 100$ , Figure 4 shows the response evolution of the closed-loop system state vector  $z(t)$  and its derivative to a unity set point and to an exogenous sinusoidal disturbance signal  $w(t) = 1000 \sin(5t) + 1000$  for  $t \in [7, 12]$  sec. It is important to mention that small impacts are observed on the dynamic response of the system for different values of the driver-plus-seat mass. Figure 5 shows close views of the evolution of the displacement on the seat,  $z_1(t)$ , and its time-derivative, according to the value of  $m_s \in [70, 120]$ . Finally, Figure 6 shows the control signal, where we can see that

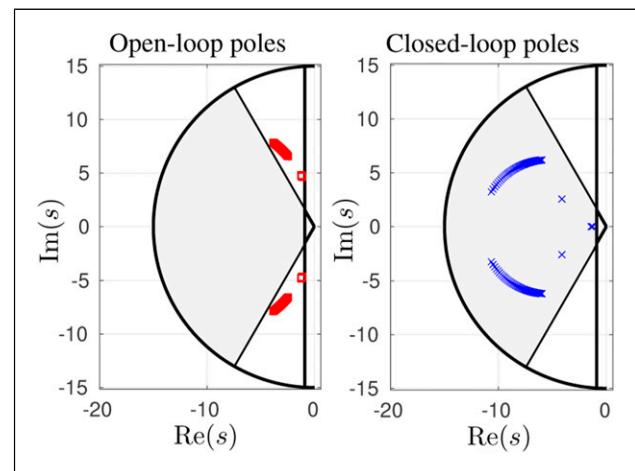


**Figure 3.** The left-hand figure shows the system open-loop poles and the right-hand one its closed-loop poles for all integer values of  $m_s$ . The shaded area indicates the desired D-region for the system closed-loop pole placement. Example 1.

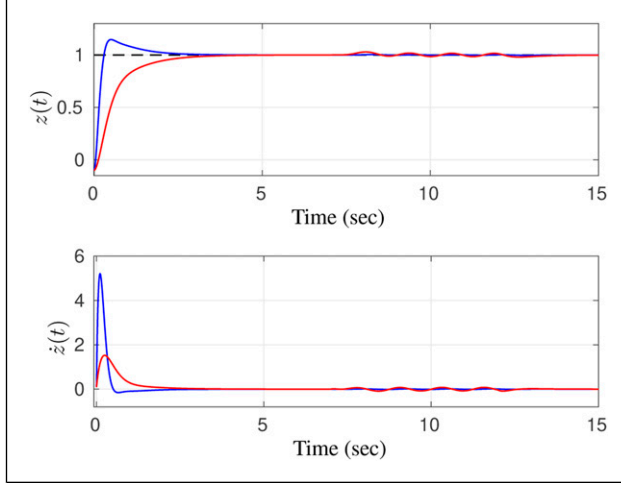


**Figure 4.** The system closed-loop response to a unity set point and to an exogenous sinusoidal disturbance signal  $w(t) = 1000 \sin(5t) + 1000$  for  $t \in [7, 12]$ sec. Example 1.

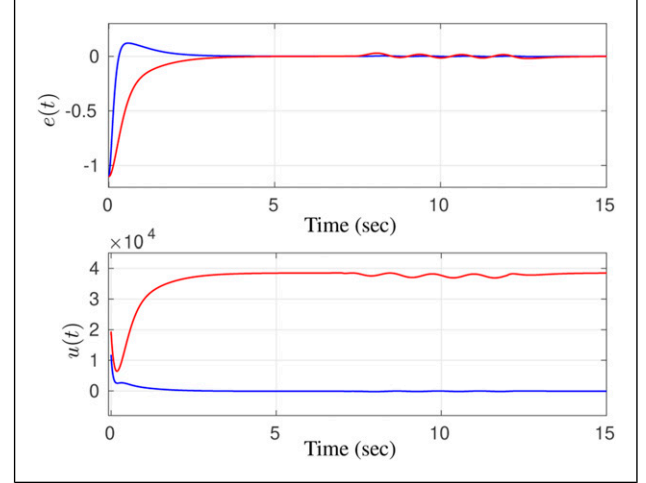


**Figure 6.** Closed-loop error response on the actuated state  $e(t)$  and control signal  $u(t)$  to a unity set point and to an exogenous sinusoidal disturbance signal  $w(t) = 1000 \sin(5t) + 1000$  for  $t \in [7, 12]$ sec, for  $m_s = 100$  kg. Example 1.

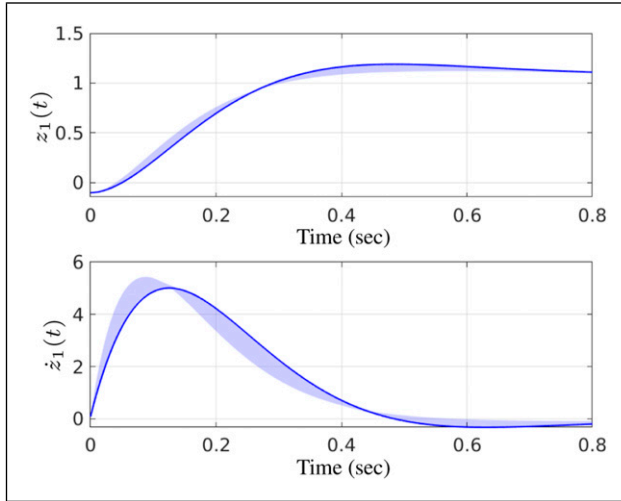


**Figure 5.** Close views of the closed-loop system states,  $z_1(t)$  and  $\dot{z}_1(t)$ , where the shaded area indicates where the signal may take place for integer values of  $m_s$ . Example 1.

it does not exceed the bound  $u_{\max}$  and the error on the actuated state reaches zero in steady-state.

**Example 2.** Consider the underactuated, singular mass four degrees-of-freedom mechanical system explored in Abdelaziz (2015), sketched in Figure 7, which dynamics model can be written as (1) with:  $M = \text{diag}\{m_1, m_2, m_3, 0\}$

$$D = \begin{bmatrix} b_1 + b_2 & -b_2 & 0 & 0 \\ -b_2 & b_2 + b_3 & -b_3 & 0 \\ 0 & -b_3 & b_3 + b_4 & -b_4 \\ 0 & 0 & -b_4 & b_4 \end{bmatrix},$$

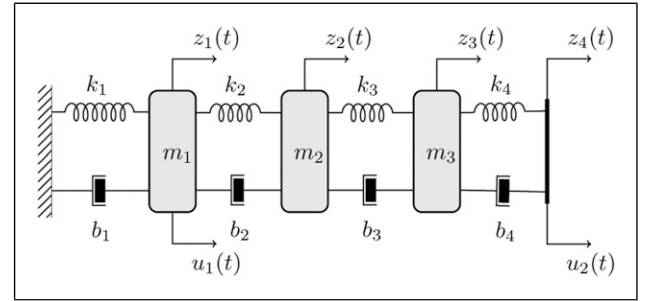


**Figure 7.** Mechanical system. Example 2.

$$S = \begin{bmatrix} k_1 + k_2 & -k_2 & 0 & 0 \\ -k_2 & k_2 + k_3 & -k_3 & 0 \\ 0 & -k_3 & k_3 + k_4 & -k_4 \\ 0 & 0 & -k_4 & k_4 \end{bmatrix},$$

$$B = \begin{bmatrix} 1 & 0 & 0 & 0 \\ 0 & 0 & 0 & 1 \end{bmatrix}^T \quad \text{and} \quad F = \text{diag}\{1, 0, 0, 1\},$$

where are assumed the physical system parameters values:  $m_1 = 3$  kg,  $m_2 = 2$  kg,  $m_3 = 1$  kg,  $b_1 = 5$  N-sec/m,  $b_2 = 10$  N-sec/m,  $b_3 = 15$  N-sec/m,  $b_4 = 20$  N-sec/m,  $k_1 = 5$  N/m,  $k_2 = 15$  N/m,  $k_3 = 15$  N/m,  $k_4 = 20$  N/m. Note that this system can be represented by (5) setting  $U = B^T$ .

Before proceeding to the controller design, note that this system presents an impulsive behavior due to an open-loop pole at infinite, see Table 1, which can result in possible harmful unwanted dynamic behaviors. Physically, the fourth degree of freedom is stressed to a jump in velocity due to its negligible mass, resulting in a mechanical shock in

**Table 1.** Open-loop and closed-loop system poles in the Example 2.

Open-loop	Closed-loop
$-\infty, -23.698,$	$-14.2587 \pm j6.2459,$
$-0.3680 \pm j0.7923,$	$-4.0065, -3.2294,$
$-1.9284, -5.0792,$	$-1.4582, -1.3700,$
$-1.0585, -1.$	$-7.2055, -5.8602,$
	$-1.2489, -1.0232.$

the connected dashpot and spring. Acceleration feedback brings the benefit of eliminating this issue. Thus, the objective of the PIDA controller proposed is to eliminate the impulsive behavior with acceleration feedback, generated by the infinite open-loop pole, and to assign for the system desired dynamic behaviors by the closed-loop pole placement.

Thus for the controller design the specifications are as follows: (i) limitation on the control signal amplitude as in (9) with  $u_{\max} = 120$  for the initial condition  $x(0) = [0.4 \ 0.4 \ 0.4 \ 0.4 \ -0.02 \ -0.02 \ -0.02 \ -0.02 \ 0.001 \ 0.001]^T$ , (ii)  $H_\infty$  disturbance attenuation level  $\gamma = 0.9010$ , and (iii) the system closed-loop pole placement in the D-region defined as the intersection of the half-plane defined by  $\text{Re}(s) < -0.9$ , a conic sector centered at the origin and with inner angle given by  $\theta = \pi/4$ , and a disk with radius  $\rho = 20$  as shown in Figure 1. Then following the steps in Procedure 1, we set  $\beta = 0.1$  in Lemma 1, that yields the PIDA controller gains

$$K_A = \begin{bmatrix} 1.2655 & 0 \\ 0 & 0 \\ 0 & 0 \\ 0 & -1.7345 \end{bmatrix}, K_P = \begin{bmatrix} -61.819 & -16.591 \\ -27.325 & 31.7718 \\ 14.2869 & -71.324 \\ -20.834 & 2.8653 \end{bmatrix}^T$$

$$K_D = \begin{bmatrix} -7.9785 & -16.5291 & 10.9827 & -10.6981 \\ -6.8143 & 29.4912 & -71.0446 & 31.8443 \end{bmatrix},$$

$$K_I = \begin{bmatrix} -75.4615 & -4.2255 \\ -9.7808 & -33.2117 \end{bmatrix}.$$

For illustration, the respective open-loop and closed-loop poles are summarized in Table 1, all closed-loop poles belong to the desired D-region as can be seen in the Figure 8. Figure 9 describes the displacement,  $z(t)$  and its derivative  $\dot{z}(t)$ , to a unity set point and to an exogenous sinusoidal disturbance signal  $w(t) = \sin(5t) + 1$  for  $t \in [10, 20]$ sec. The displacement error paths  $e_d(t)$  and the input signal  $u(t)$ , for the two actuated states, can be seen in Figure 10, where the maximum limit value  $u_{\max}$  is respected.

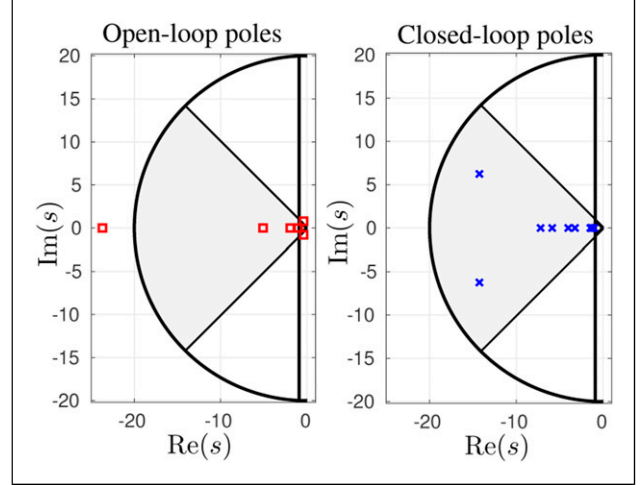


**Figure 8.** The left-hand figure shows the system finite open-loop poles and the right-hand one its closed-loop poles. The shaded area indicates the desired D-region for the system closed-loop pole placement. Example 2.

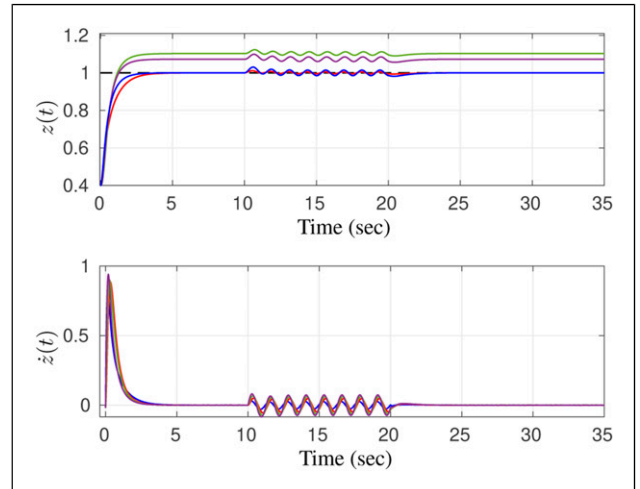


**Figure 9.** The system closed-loop response to a unity set point and to an exogenous sinusoidal disturbance signal  $w(t) = \sin(5t) + 1$  for  $t \in [10, 20]$ sec. Example 2.

**Example 3.** In this example, the proposed approach is applied on a set-point tracking control for a nonlinear system. We borrowed from Lipták et al. (2017) the model of a flexible rotor coupled to an arm link, sketched in Figure 11. The system consists of a rotor actuated by the torque generated with a motor, where the degrees-of-freedom are the angles in the two extreme points of the rotor:  $\varphi_1(t)$  in the side coupled to the link and  $\varphi_2(t)$  in the side driven by the motor. A non-linearity of sweep-pendulum type can be noticed in the dynamical



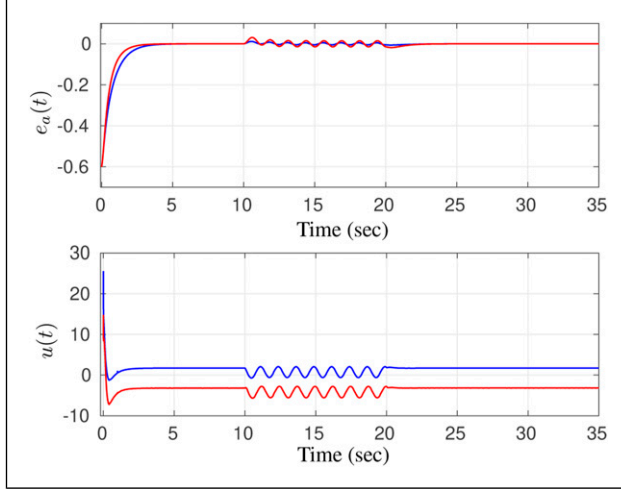


**Figure 10.** Closed-loop error response on the actuated state vector  $e_a(t)$  and control signal  $u(t)$  to a unity set point and to an exogenous sinusoidal disturbance signal  $w(t) = \sin(5t) + 1$  for  $t \in [10, 20]$ sec. Example 2.

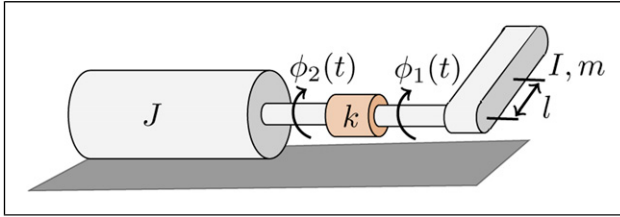


**Figure 11.** Flexible rotor coupled to an arm link. Example 3.

equations of the system derived by the Euler–Lagrange formulation

$$\begin{aligned} I\ddot{\phi}_1(t) + mgl \sin(\phi_1(t)) + k[\phi_1(t) - \phi_2(t)] &= 0 \\ J\ddot{\phi}_2 + k[\phi_2(t) - \phi_1(t)] &= u(t) \end{aligned} \quad (18)$$

Denoting the nonlinear term as

$$\sin(\phi_1(t)) = \phi_1(t) \operatorname{sinc}(\phi_1(t)), \quad (19)$$

the system time-varying stiffness matrix is given by

$$S(t) = \begin{bmatrix} k + mgl \operatorname{sinc}(\phi_1(t)) & -k \\ -k & k \end{bmatrix}. \quad (20)$$

Now assuming that the swing angle of the link belongs in the interval  $\phi_1(t) \in [-\frac{\pi}{2}, \frac{\pi}{2}]$ , such that  $\operatorname{sinc}(\phi_1(t)) \in [\frac{2}{\pi}, 1]$ , considering the nonlinear term in  $\phi_1(t)$  as the source of uncertainty for the system dynamics and setting values for the system parameters:  $l = 0.1$ ,  $m = 1$ ,  $I = 0.05$ ,  $J = 0.1$ ,  $g = 10$ ,  $k = 50$ . This setup allows us to describe the system dynamics by an uncertain second-order linear model whose matrices belong to the polytopic set in (2) with vertices

$$M_1 = M_2 = \begin{bmatrix} 0.05 & 0 \\ 0 & 0.1 \end{bmatrix}, D_1 = D_2 = \begin{bmatrix} 0 & 0 \\ 0 & 0 \end{bmatrix},$$

$$S_1 = \begin{bmatrix} 51 & -50 \\ -50 & 50 \end{bmatrix}, S_2 = \begin{bmatrix} 50.64 & -50 \\ -50 & 50 \end{bmatrix},$$

$$B_1 = B_2 = \begin{bmatrix} 0 & 1 \end{bmatrix}^T.$$

Thus, with the controller design specifications: system closed-loop pole placement in the D-region defined as the intersection of the half-plane defined by  $\operatorname{Re}(s) < -5$ , a conic sector centered at the origin and with inner angle given by  $\theta = \pi/3$ , and a disk with radius  $\rho = 15$  as shown in Figure 1. The Procedure 1 yields the PID controller gains

**Table 2.** Open-loop and closed-loop system poles at its vertices, Example 3.

$\phi_1(t)$	Open-loop	Closed-loop
$-\frac{\pi}{2}$	$\pm 38.9023j$ , $\pm 2.5705j$	$-8.0620 \pm 11.9675j$ , $-13.5952$ , $-5.7727 \pm 4.0952j$ .
$\frac{\pi}{2}$	$\pm 38.8396j$ , $\pm 2.0543j$	$-6.8103 \pm 9.9304j$ , $-5.9872$ , $-10.8284 \pm 6.7034j$ .

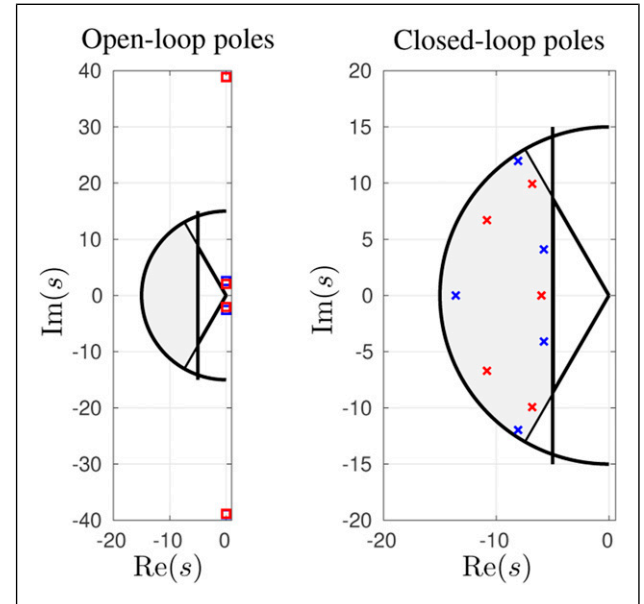


**Figure 12.** The left-hand figure shows the system finite open-loop poles and the right-hand one its closed-loop poles. The shaded area indicates the desired D-region for the system closed-loop pole placement. Example 3.

$$K_P = [-75.7438 \quad 69.9357], K_D = [3.2975 \quad -4.1265],$$

$$K_I = -13.9027.$$

For the results analysis purposes, the open and closed-loop system poles at its vertices are summarized in Table 2. All closed-loop poles belong to the desired D-region as can be seen in the Figure 12. Figure 13 shows the response evolution of the closed-loop system state vector  $z(t)$  and its derivative  $\dot{z}(t)$  to a piece-wise constant set-point (dashed line) on the actuated degree of freedom. The displacement error paths  $e_a(t)$  and the input signal  $u(t)$ , can be seen in Figure 14. One can notice that the reference tracking depicts the expected response despite the nonlinear effect induced

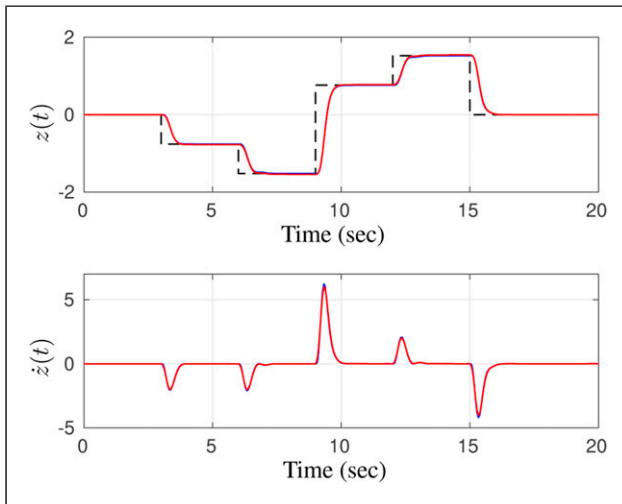


**Figure 13.** The system closed-loop response to a piece-wise constant set-point. Example 3.

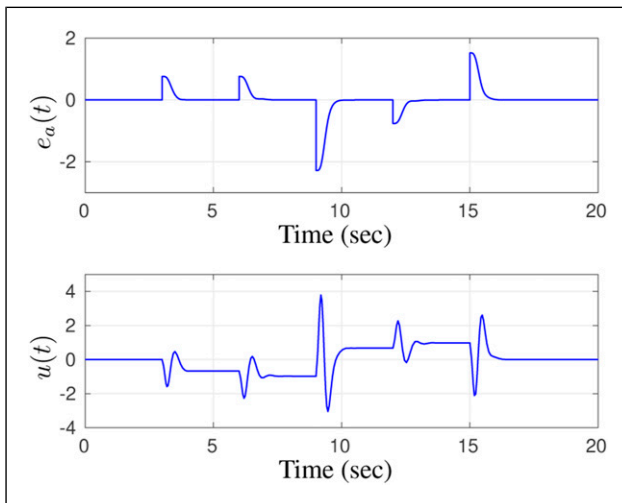


**Figure 14.** Closed-loop error response on the actuated state vector  $e_a(t)$  and control signal  $u(t)$ . Example 3.

by the significant excursion range beyond the original rest positioning.

### 3. Conclusion

A robust framework to design multivariable PID and PIDA controllers has been proposed in order to control vibrating systems modeled by second-order differential equations. The integral action provides an additional design flexibility, which is explored to improve closed-loop performance based on LMI optimization and to achieve offset-free tracking of the actuated degrees-of-freedom in the presence of constant reference and disturbances. Moreover, the acceleration action is proposed to solve the regularization problem. One of the main benefits of the proposed framework comes from the fact that the design approach is systematic. Hence, integral and the acceleration gains bring no relevant drawback with respect to design complexity, despite the benefits with respect to performance improvement, reference tracking property and regularization effect. Practical challenges for mechanical systems such as  $H_\infty$  performance optimization, regional pole placement, and saturation avoidance can be handled jointly despite the modeling error. The conservativeness of the difference polytopic inclusion in the context of the PIDA design with respect to the delays and nonlinear uncertainties is an interesting topic for further investigation.

### Declaration of conflicting interests

The author(s) declared no potential conflicts of interest with respect to the research, authorship, and/or publication of this article.


### Funding

The author(s) disclosed receipt of the following financial support for the research, authorship, and/or publication of this article: This study was financed in part by the Coordenação de Aperfeiçoamento de Pessoal de Nível Superior—Brasil (CAPES) - Finance Codes 001, Conselho Nacional de Desenvolvimento Científico e Tecnológico - Brasil (CNPq: 429 819/2 018-8 and 312 034/2 020-2), and Fundação de Amparo à Pesquisa do Estado de Minas Gerais - Brasil (FAPEMIG: APQ-00 543-17).

### ORCID iDs

Danielle S Gontijo  <https://orcid.org/0000-0002-9047-1396>

José M Araújo  <https://orcid.org/0000-0002-4170-7067>

Fernando O Souza  <https://orcid.org/0000-0002-8634-4810>

### References

- Abdelaziz TH (2013) Robust pole placement for second-order linear systems using velocity-plus-acceleration feedback. *IET Control Theory and Applications* 7(14): 1843–1856.

- Abdelaziz TH (2015) Robust pole assignment using velocity–acceleration feedback for second-order dynamical systems with singular mass matrix. *ISA Transactions* 57: 71–84.
- Acevedo M, Orvaños Guerrero MT and Velázquez R et al. (2020) An alternative method for shaking force balancing of the 3RRR PPM through acceleration control of the center of mass. *Applied Sciences* 10(4): 1351.
- Adamson LJ, Fichera S and Mottershead JE (2020) Receptance-based robust eigenstructure assignment. *Mechanical Systems and Signal Processing* 140: 106697.
- Alfadhli A, Darling J and Hillis AJ (2018) The control of an active seat with vehicle suspension preview information. *Journal of Vibration and Control* 24(8): 1412–1426.
- Araújo JM, Dórea CET and Gonçalves LMG et al. (2018) Robustness of the quadratic partial eigenvalue assignment using spectrum sensitivities for state and derivative feedback designs. *Journal of Low Frequency Noise, Vibration & Active Control* 37(2): 253–268.
- Bender D and Laub A (1987) The linear-quadratic optimal regulator for descriptor systems. *IEEE Transactions on Automatic Control* 32(8): 672–688.
- Boyd S, Ghaoui LE and Feron E et al. (1994) *Linear matrix inequalities in system and control theory*. Philadelphia, Pa: Society for Industrial and Applied Mathematics.
- Cai Y-F, Qian J and Xu S-F (2010) The formulation and numerical method for partial quadratic eigenvalue assignment problems. *Numerical Linear Algebra with Applications* 18(4): 637–652.
- Chilali M and Gahinet P (1996)  $H_\infty$  design with pole placement constraints: an LMI approach. *IEEE Transactions on Automatic Control* 41(3): 358–367.
- Datta S (2017) Feedback controller norm optimization for linear time invariant descriptor systems with pole region constraint. *IEEE Transactions on Automatic Control* 62(6): 2794–2806.
- de Almeida MO and Araújo JM (2019) Partial eigenvalue assignment for LTI systems with D-stability and LMI. *Journal of Control* 30: 2195–3899.
- Franklin TS, Araújo JM and Santos TL (2021) Receptance-based robust stability criteria for second-order linear systems with time-varying delay and unstructured uncertainties. *Mechanical Systems and Signal Processing* 149: 107191.
- Gielen RH, Olaru S and Lazar M et al. (2010) On polytopic inclusions as a modeling framework for systems with time-varying delays. *Automatica* 46(3): 615–619.
- Gudarzi M (2015)  $\mu$ -synthesis controller design for seismic alleviation of structures with parametric uncertainties. *Journal of Low Frequency Noise, Vibration and Active Control* 34(4): 491–511.
- Guo J, Wang J and Luo Y et al. (2020) Robust lateral control of autonomous four-wheel independent drive electric vehicles considering the roll effects and actuator faults. *Mechanical Systems and Signal Processing* 143: 106773.
- Hayati H, Eager D and Pendrill AM et al. (2020) Jerk within the context of science and engineering—a systematic review. *Vibration* 3(4): 371–409.
- Hiramoto K and Grigoriadis KM (2016) Active/semi-active hybrid control for motion and vibration control of mechanical and structural systems. *Journal of Vibration and Control* 22(11): 2704–2718.
- Hu T, Teel AR and Zaccarian L (2006) Stability and performance for saturated systems via quadratic and nonquadratic Lyapunov functions. *IEEE Transactions on Automatic Control* 51(11): 1770–1786.
- Li H, Liu H and Hilton C et al. (2013) Non-fragile  $H_\infty$  control for half-vehicle active suspension systems with actuator uncertainties. *Journal of Vibration and Control* 19(4): 560–575.
- Lipták T, Kelemen M and Gmiterko A et al. (2017) Input-state linearization of mechanical system. *American Journal of Mechanical Engineering* 5(6): 298–302.
- Mottershead JE, Tehrani MG and James S et al. (2008) Active vibration suppression by pole-zero placement using measured receptances. *Journal of Sound and Vibration* 311(3): 1391–1408.
- Pan H and Sun W (2019) Nonlinear output feedback finite-time control for vehicle active suspension systems. *IEEE Transactions on Industrial Informatics* 15(4): 2073–2082.
- Ram YM and Mottershead JE (2013) Multiple-input active vibration control by partial pole placement using the method of receptances. *Mechanical Systems and Signal Processing* 40(2): 727–735.
- Reithmeier E and Leitmann G (2003) Robust vibration control of dynamical systems based on the derivative of the state. *Archive of Applied Mechanics* 72(11): 856–864.
- Richiedi D and Tamellini I (2021) Active control of linear vibrating systems for antiresonance assignment with regional pole placement. *Journal of Sound and Vibration* 494: 115858.
- Singh KV, Black C and Kolonay R (2019) Active aeroelastic output feedback control with partial measurements by the method of receptances. *Aerospace Science and Technology* 86: 47–63.
- Sun W, Gao H and Kaynak O (2015) Vibration isolation for active suspensions with performance constraints and actuator saturation. *IEEE/ASME Transactions on Mechatronics* 20(2): 675–683.
- Tu L, Du H and Dong M et al. (2021) Semiactively controllable vehicle seat suspension system with negative stiffness magnetic spring. *IEEE/ASME Transactions on Mechatronics* 26(1): 156–167.
- Xie H (2021) A receptance method for robust and minimum norm partial quadratic eigenvalue assignment. *Mechanical Systems and Signal Processing* 160: 107838.
- Zhang SQ, Li HN and Schmidt R et al. (2014) Disturbance rejection control for vibration suppression of piezoelectric laminated thin-walled structures. *Journal of Sound and Vibration* 333(5): 1209–1223.
- Zhang S-Q, Zhang X-Y and Ji H-L et al. (2021) A refined disturbance rejection control for vibration suppression of smart structures under unknown disturbances. *Journal of Low Frequency Noise, Vibration and Active Control* 40(1): 427–441.
- Zhang T and Li HG (2013) Adaptive pole placement control for vibration control of a smart cantilevered beam in thermal environment. *Journal of Vibration and Control* 19(10): 1460–1470.
- Zhang X-Y, Zhang S-Q and Wang Z-X et al. (2019) Disturbance rejection control with  $H_\infty$  optimized observer for vibration suppression of piezoelectric smart structures. *Mechanics & Industry* 20(2): 202.
- Zhu J, Mottershead JE and Kyprianou A (2009) An inverse method to assign receptances by using classical vibration absorbers. *Journal of Vibration and Control* 15(1): 53–84.